

# Quaternary tungsten-based alloys as plasma-facing material for fusion reactors

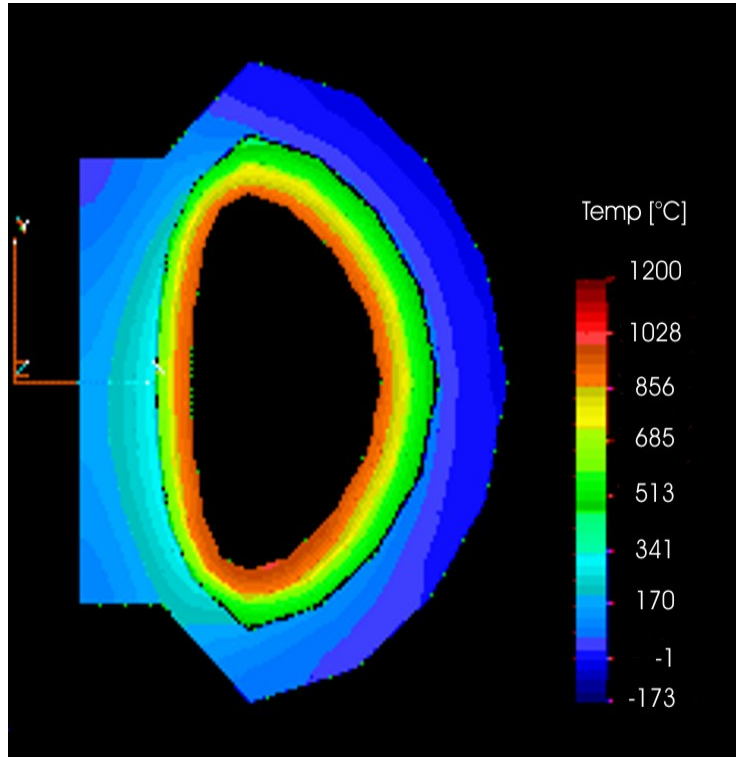
**Christian Linsmeier**

**F. Koch, C. Lenser, M. Balden,  
M. Rasinski**

*Max-Planck-Institut für Plasmaphysik,  
Garching b. München, Germany*

- Applications: DEMO (and ITER)
- Self-passivation mechanism
- Characterization of quaternary alloys
- Summary

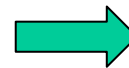
## Power plant conceptual study



*Temperature profile in PPCS Model A, 10 days after accident with a total loss of all coolant.*

*[Final Report of the European Fusion Power Plant Conceptual Study, 2004]*

- Accidental loss of coolant: peak temperatures of first wall up to 1200 °C due to nuclear afterheat
- Additional air ingress: formation of highly volatile  $\text{WO}_3$
- Evaporation rate: order of 10 -100 kg/h at  $>1000^\circ\text{C}$  in a reactor (1000 m<sup>2</sup> surface)  
→ large fraction of radioactive  $\text{WO}_3$  may leave hot vessel



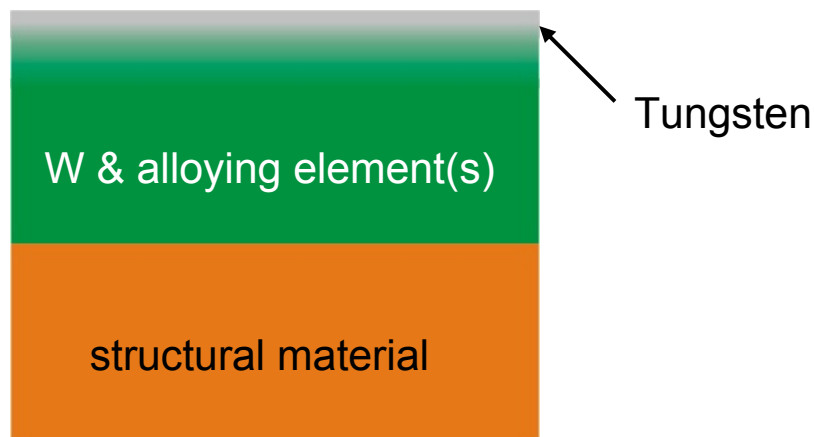
Development of self-passivating tungsten alloys

## Self passivating tungsten-based alloys:

Surface composition automatically adjusts to the requested property

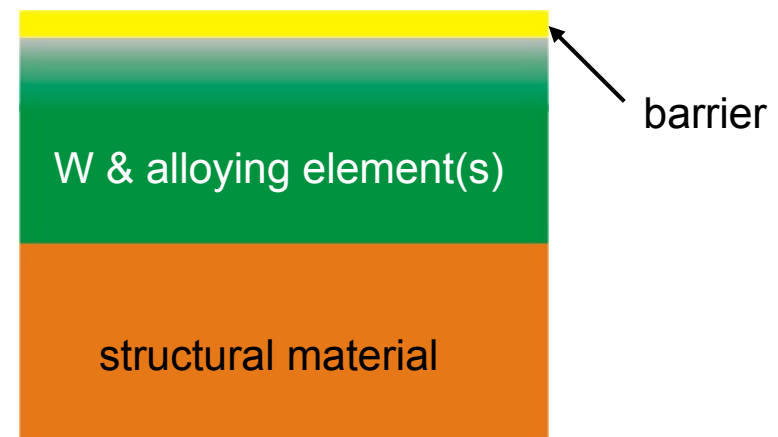
### Normal operation (600°C):

Formation of tungsten surface by depletion of alloying element(s) due to preferential sputtering



### Accidental conditions:

(air ingress, up to 1200 °C)  
Formation of protective barrier layer

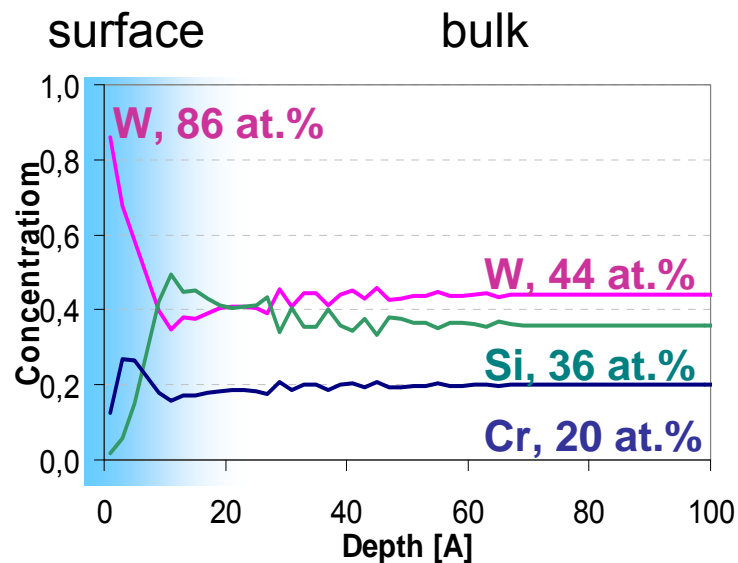


## Self passivating tungsten-based alloys:

Surface composition automatically adjusts to the requested property

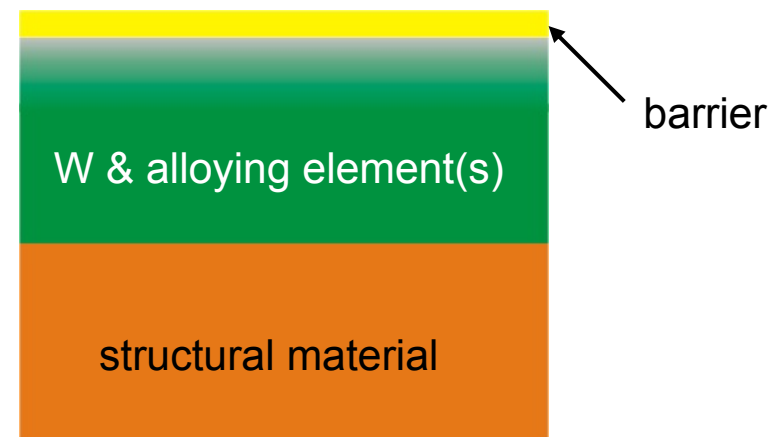
### Normal operation (600°C):

TRIDYN numerical simulation of sputter erosion of W-Si-Cr alloy (D ions, 30 eV, fluence  $10^{18}/\text{cm}^2$ )



### Accidental conditions:

(air ingress, up to 1200 °C)  
Formation of protective barrier layer

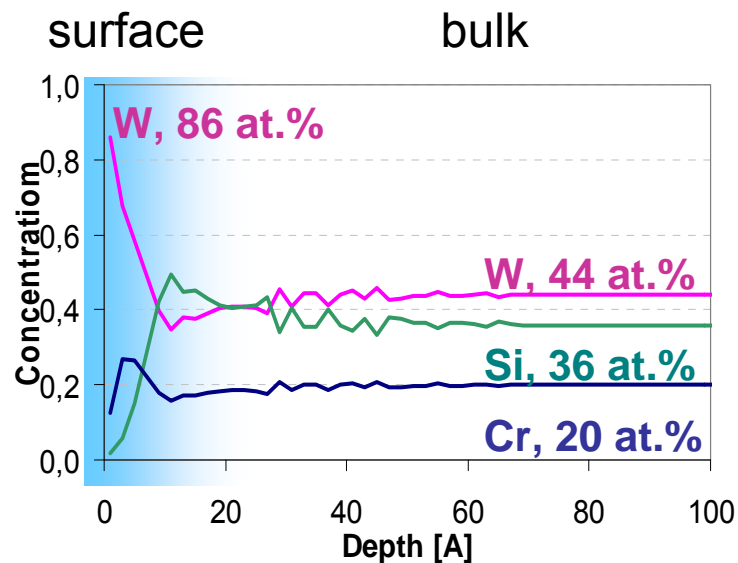


## Self passivating tungsten-based alloys:

Surface composition automatically adjusts to the requested property

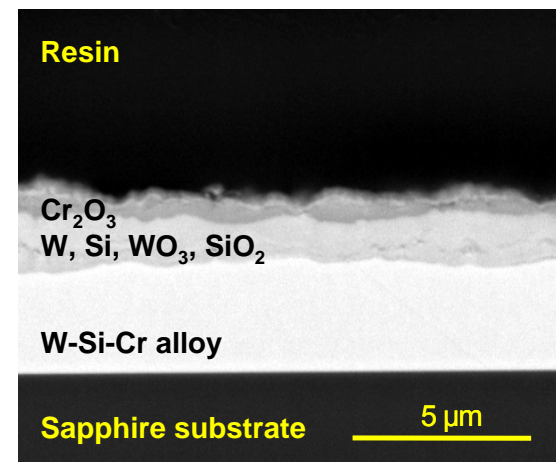
### Normal operation (600°C):

TRIDYN numerical simulation of sputter erosion of W-Si-Cr alloy (D ions, 30 eV, fluence  $10^{18}/\text{cm}^2$ )



### Accidental conditions:

Cross section of sputter deposited W-Si-Cr film after oxidation at 1000°C for 1h



Addition of reactive elements to W-Si-Cr to improve oxide film formation and adherence

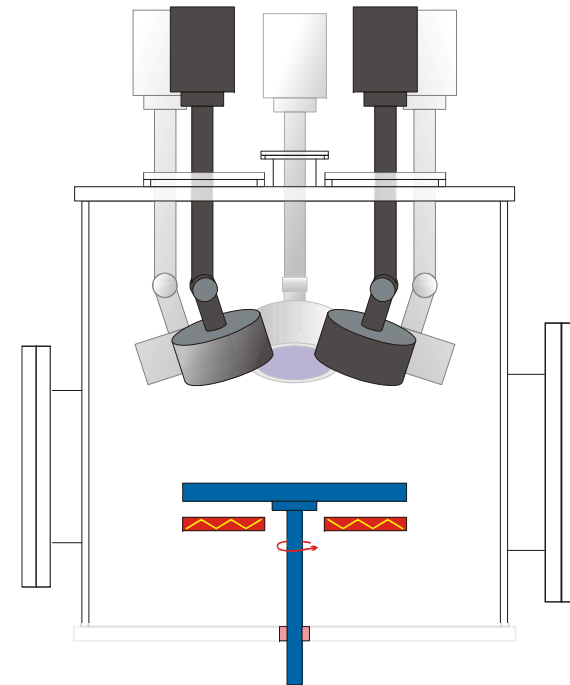
## Co-deposition by Magnetron Sputtering

- Film thickness  $\sim 4\mu\text{m}$
- $\text{SiO}_2$  and  $\text{Al}_2\text{O}_3$  substrates used for oxidation

### Investigated systems

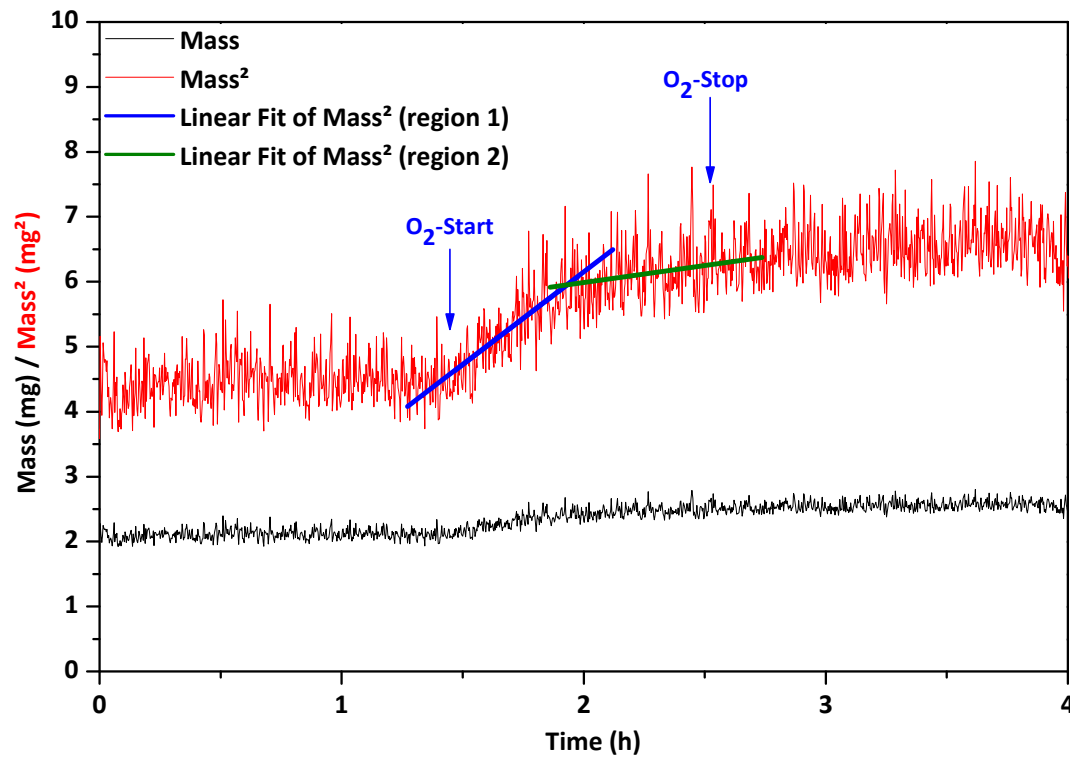
- W-Si-Cr-Zr
- W-Si-Cr-Y

(different concentrations)



Schematic view of deposition facility

## Oxidation of W-Si4-Cr8-Y3 at 1000°C for 1 hours



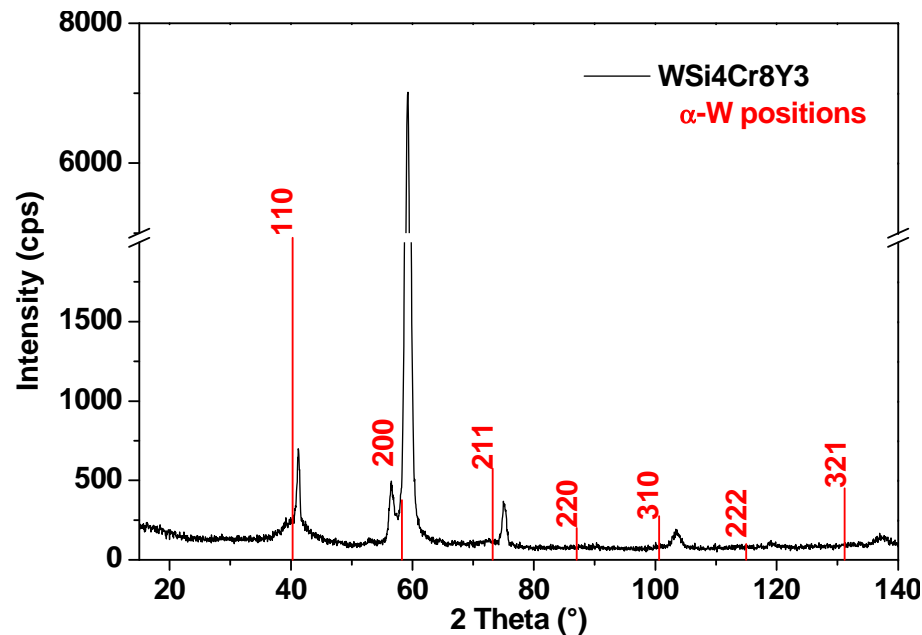
- Heating under inert gas flow
- Start of oxygen at stable temperature

- Parabolic oxidation rates:  $(\Delta m)^2 = k t$ : → Diffusion-governed process
- Two distinct oxidation rates



# XRD analysis: alloys as deposited

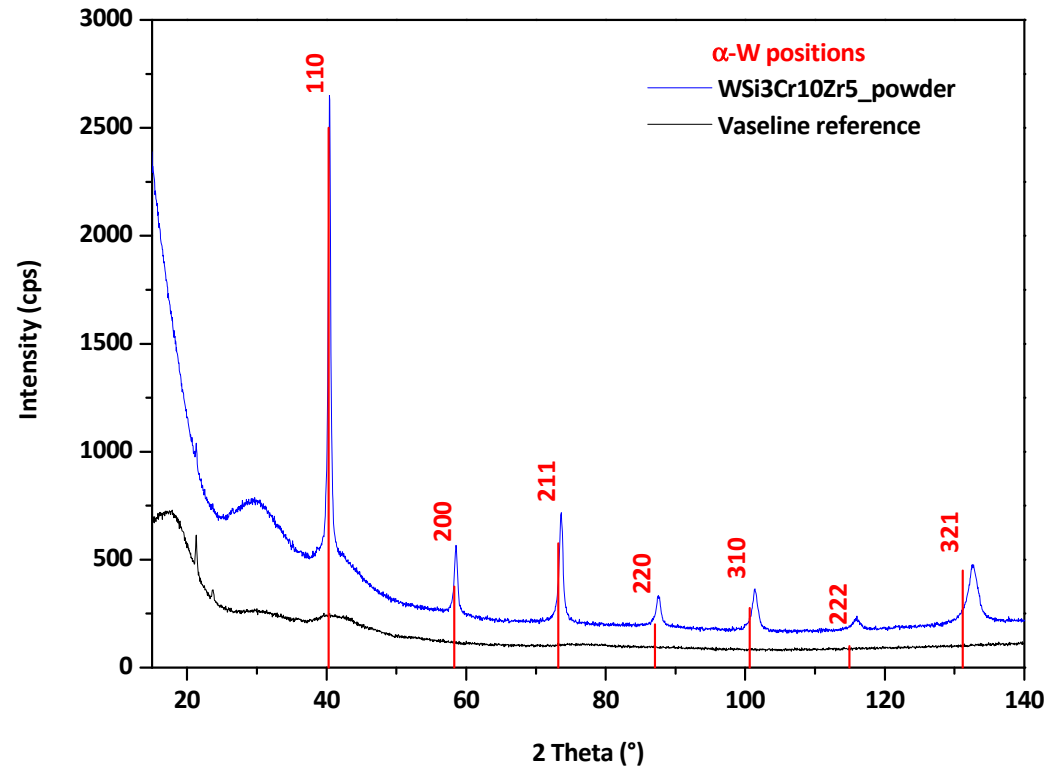
## Peak shift due to Lattice Distortion



$d$	$2\theta$	$h$	$k$	$l$
Angström	°			
2,2976	39.177	1	1	0
2,1922	41.1438	1	1	0
1,5567	59.3162	2	0	0
1,3043	72.3989	2	1	1
1,2668	74.8987	2	1	1
0,9823	103.2851	3	1	0
0,8283	136.8753	3	2	1

- Fifth order polynomial by Gust *et al.* used to calculate W concentration in assumed binary W-Cr lattice
- $c(\text{Cr}) = 27.5$  at-% from peak shift;  $c(\text{Cr}) = 29.2$  at-% from RBS

Gust, W.; Predel, B.; Roll, U.: Journal of the Less-Common Metals, 69, pp. 331-353, 1980

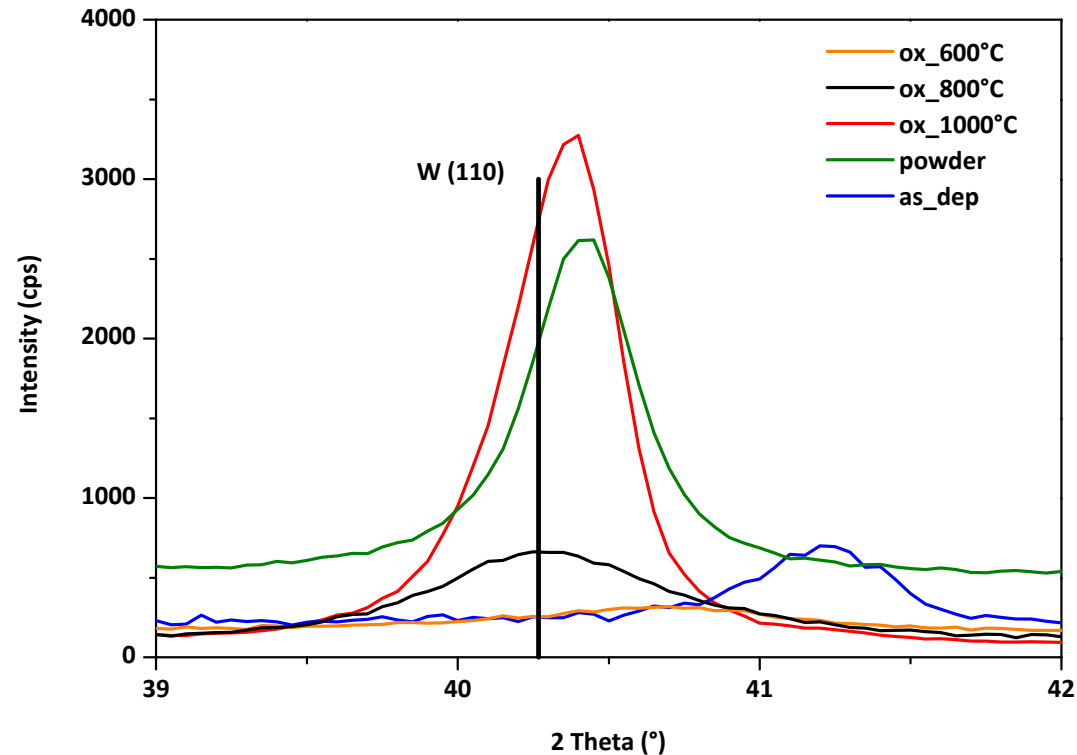


## WSi<sub>3</sub>Cr<sub>10</sub>Zr<sub>5</sub> powder

(annealed at 1000 °C under Ar)

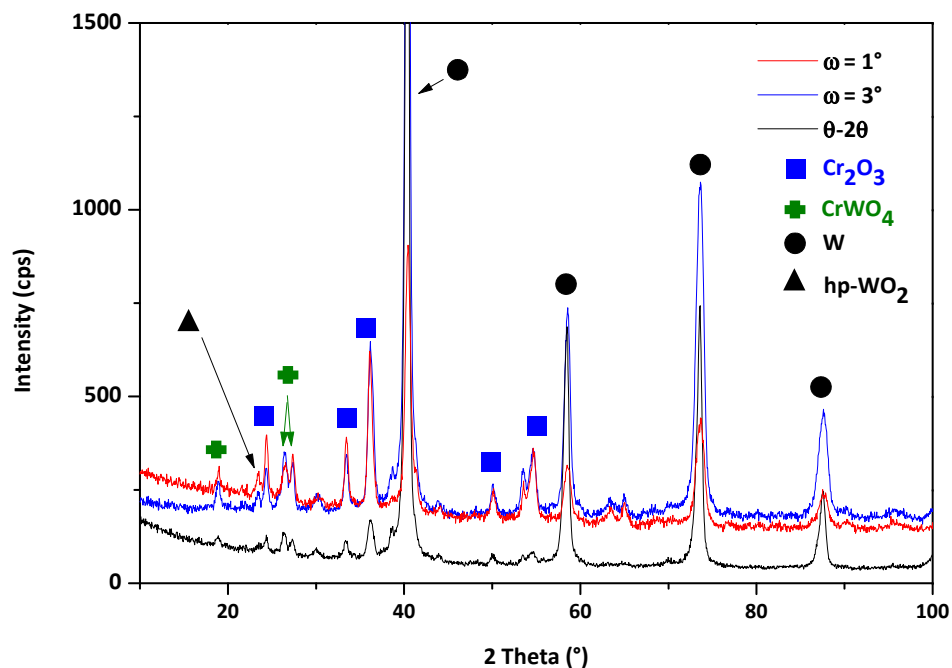
- c(Cr) = 24 at-% after deposition (RBS); c(Cr) = 6.75 at-% after annealing
- Thermodynamic equilibrium: c(Cr) = 7 at-% (Gust et al.)
- Cr precipitates from the binary lattice

## WSi3Cr10Zr5



- Lattice shows strongest distortion after deposition
- Equilibrium concentration of Cr in W lattice is reached at 800°C and 1000°C, but not at 600°C
- Powder has virtually the same peak shift as film -> not stress-related

# XRD analysis: oxidized alloys



WSi<sub>3</sub>Cr<sub>10</sub>Zr<sub>5</sub> (oxidized 1h at 1000 °C)

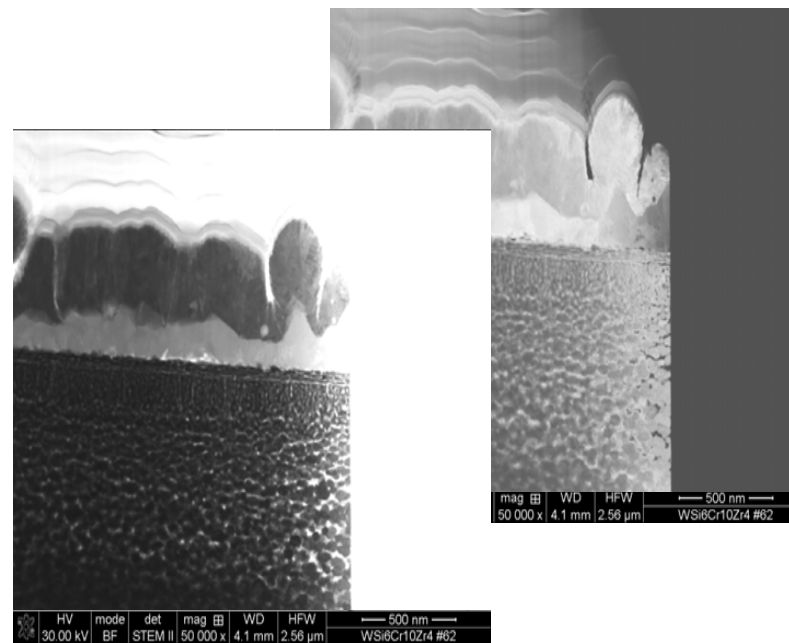
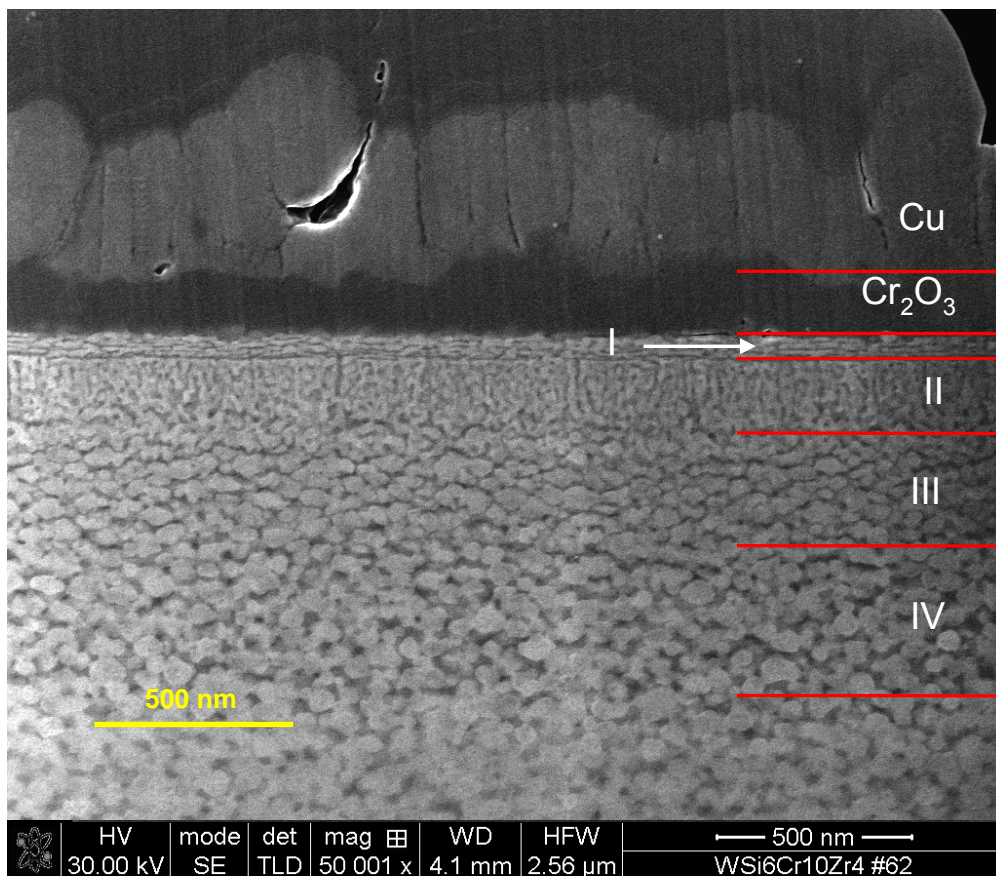
## Phases identified by XRD

Ox. temp.	600°C	800°C	1000°C
Ox. time	48 h	4 h	1 h
	Cr <sub>2</sub> O <sub>3</sub>	Cr <sub>2</sub> O <sub>3</sub>	Cr <sub>2</sub> O <sub>3</sub>
	CrWO <sub>4</sub>	CrWO <sub>4</sub>	CrWO <sub>4</sub>
	W	W	W
	WO <sub>2</sub>	WO <sub>2</sub>	
	hp-WO <sub>2</sub>	hp-WO <sub>2</sub>	hp-WO <sub>2</sub>
	ZrSiO <sub>4</sub>		

→ no volatile WO<sub>3</sub> formed!

# Microstructure of oxidized alloys

## WSi3Cr10Zr5:



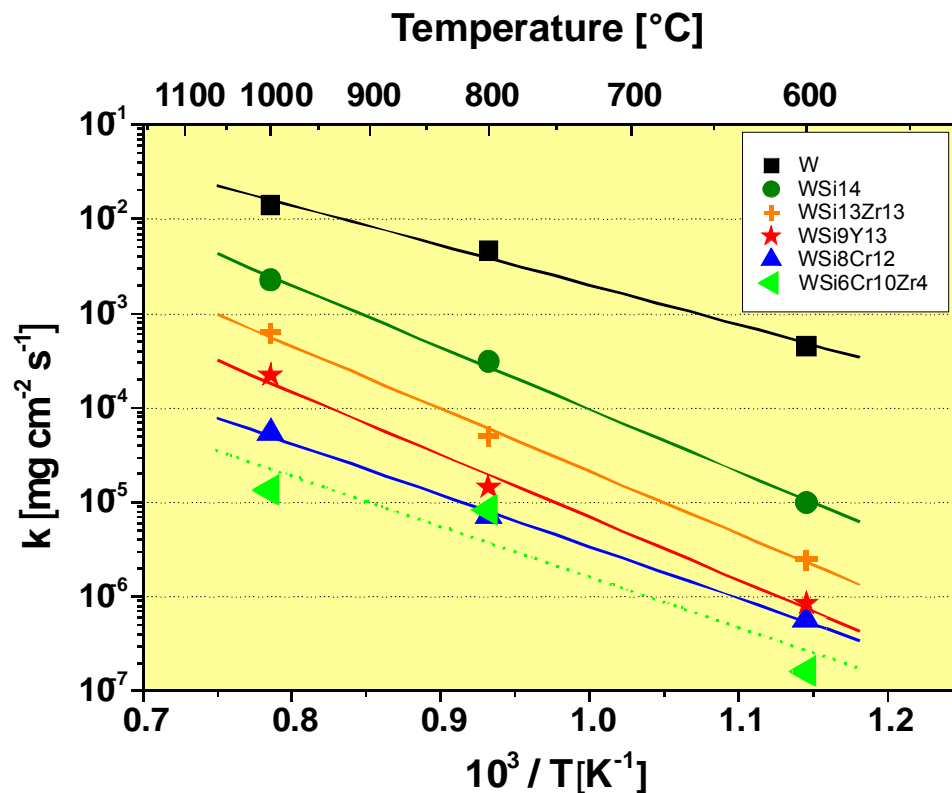
- Dense  $\text{Cr}_2\text{O}_3$  barrier scale
- Cr is main diffusing species
- Mixed oxide zone(s)
- Cr depletion zone with voids
- No formation of  $\text{WO}_3$

**SEM of cross section (FIB), 1000°C, 1h**

# Comparison of oxidation results



## Arrhenius plot of oxidation rates of tungsten and tungsten alloys



Oxidation rate (k) has been calculated from weight increase versus time, linear fit.

Alloy	W	Si	Cr	Zr
WSi8Cr12	46	30	24	-
WSi3Cr10Zr5	56	13	24	7

Composition in at.%

Linear oxidation rates of W-Si-Cr & quaternary alloys comparable.

Quaternary alloys show distinct parabolic oxidation behavior at reduced level of alloying elements.

## Conclusions quaternary alloys:

- **Quaternary alloys** show better passivation behavior than ternary while **containing more W**
- Active elements (Y/Zr) do not form oxide layers, but **improve oxide scale adhesion**
- Surface oxide consists of **Cr<sub>2</sub>O<sub>3</sub>**
- Oxide phases formed are Cr<sub>2</sub>O<sub>3</sub>, WCrO<sub>4</sub>, WO<sub>2</sub> (2 modifications), ZrSiO<sub>4</sub> (600°C), but **no WO<sub>3</sub> → passivation successful**
- **Two step-oxidation**: switch in oxidation mechanism during oxidation
- Different oxidation **mechanisms** at different **temperatures**
- Restructuring induced by the **precipitation of Cr from the W lattice**